AD-A258 331

IMENTATION PAGE

Form Approved
OMB No. 0704-0188

s estimated to average 1 hour per response, including the time for reviewing instructions, searching existing data sources, ting and reviewing the collection of information. Send comments regarding this burden estimate or any other aspect of this cing this burden to Washington Headquarters Services, Directorate for information Operations and Reports, 1215 Jefferson ns to the Office of Management and Budget, Paperwork Reduction Project (0704-0188), Washington, DC 20503.

2. REPORT DATE	3. REPORT TYPE AND DATES COVERED
June 12, 1992	Technical — 5/31/91 – 6/30/92

4. TITLE AND SUBTITLE "POLY(ETHYLENE OXIDE)-BASED Zn(II) HALIDE ELECTROLYTES"

5. FUNDING NUMBERS
G—N00014-90-J-1559

6. AUTHOR(S)
H. Yang and G.C. Farrington

7. PERFORMING ORGANIZATION NAME(S) AND ADDRESS(ES)
University of Pennsylvania
Department of Chemistry
Philadelphia, PA 19104-6323

8. PERFORMING ORGANIZATION REPORT NUMBER
1992-24

9. SPONSORING / MONITORING AGENCY NAME(S) AND ADDRESS(ES)

Sponsoring Agency:	Monitoring Agency:
DARPA	ONR
3701 N. Fairfax Drive	800 N. Quincy Street
Arlington, VA 22203-1714	Arlington, VA 22217-5000

10. SPONSORING / MONITORING AGENCY REPORT NUMBER

11. SUPPLEMENTARY NOTES

12a. DISTRIBUTION / AVAILABILITY STATEMENT
Distribution Unlimited

DISTRIBUTION STATEMENT A
Approved for public release;
Distribution Unlimited

12b. DISTRIBUTION CODE

13. ABSTRACT *(Maximum 200 words)*

Poly(ethylene oxide) (PEO)-based Zn(II) halide electrolytes with optimized compositions exhibit rather high conductivities compared to other PEO solutions of divalent cation salts. Chemical diffusion studies have clearly demonstrated that both Zn(II) and Br(–I) are mobile. It appears that Zn(II) cations occur in two forms, one associated with the ether oxygens and another associated with the anions. It is reasonable that the former should be less mobile than the latter. Regrettably, quantitative measurement of the transference number and diffusion coefficients of the charge carriers using elecrochemical techniques proved difficult. Other measurements found that the value of Tg for the completely amorphous forms of the electrolytes increases linearly with the mole ration of $\frac{[Zn]}{[O]}$, indicating that Zn(II) cations interact with ether oxygens in the PEO chains to form inter- and/or intrachain cross-links.

DTIC
ELECTE
DEC 09 1992
S B D

92-31115

14. SUBJECT TERMS
Poly(ethylene oxide), Zn(II) halide electrolytes, divalent cation salts, cations, anions, mole ration, transference number, diffusion coefficients, charge carriers, interchain and intrachain cross-links

15. NUMBER OF PAGES
40

16. PRICE CODE

17. SECURITY CLASSIFICATION OF REPORT	18. SECURITY CLASSIFICATION OF THIS PAGE	19. SECURITY CLASSIFICATION OF ABSTRACT	20. LIMITATION OF ABSTRACT
Unclassified	Unclassified	Unclassified	UL

OFFICE OF NAVAL RESEARCH

GRANT NO.: N00014-90-J-1559

R & T CODE NO.: A400004DF3

TECHNICAL REPORT NO.: 1992-24

"POLY(ETHYLENE OXIDE)-BASED Zn(II) HALIDE ELECTROLYTES"

by

H. Yang and G.C. Farrington

Accepted for Publication in
J. Electrochem. Soc. (1991)

University of Pennsylvania
Department of Chemistry
Philadelphia, PA 19104-6323

June 12, 1992

Reproduction in whole or in part is permitted for any purpose of the United States Government.

This document has been approved for public release and sale; its distribution is unlimited.

Poly(ethylene oxide)-based Zn(II) Halide Electrolytes

H. Yang and G. C. Farrington
Department of Materials Science and Engineering
University of Pennsylvania
3231 Walnut Street
Philadelphia, PA 19104 USA

Abstract

Poly(ethylene oxide) (PEO)-based Zn(II) halide electrolytes with optimized compositions exhibit rather high conductivities compared to other PEO solutions of divalent cation salts. Chemical diffusion studies have clearly demonstrated that both Zn(II) and Br(-I) are mobile. It appears that Zn(II) cations occur in two forms, one associated with the ether oxygens and another associated with the anions. It is reasonable that the former should be less mobile than the latter. Regrettably, quantitative measurement of the transference number and diffusion coefficients of the charge carriers using electrochemical techniques proved difficult. Other measurements found that the value of T_g for the completely amorphous forms of the electrolytes increases linearly with the mole ration of $\frac{[Zn]}{[O]}$, indicating that Zn(II) cations interact with ether oxygens in the PEO chains to form inter- and/or intrachain crosslinks.

[REVISED JES No. 91-09-042]

Accession For
NTIS GRA&I ☑
DTIC TAB ☐
Unannounced ☐
Justification
By
Distribution/
Availability Codes
Dist | Avail and/or Special
A-1

1. Introduction

High molecular weight (typically $5x10^6$) poly(ethylene oxide) (PEO) has an exceptional ability to solvate ionic salts [1] to form solid polymer electrolytes. Initial studies of these materials have focused on PEO-based Li(I) electrolytes [1,2], but more recent investigations have shown that PEO dissolves a wide range of salts of monovalent, divalent, and trivalent cations [3]. The rich coordination chemistry and spectroscopy of many multivalent ions provides better opportunities for studying the fundamental aspects of ion conduction in polymer electrolytes than do Li(I) conductors. In this paper, the general characteristics of pure PEO-based Zn(II) electrolytes, including thermal stability, phase transitions, electrical properties and electrochemical behavior, are discussed.

2. Sample Preparation

All samples were prepared by solution-casting from the starting materials listed in Table 1. Stoichiometric amounts of salts and PEO were dissolved in ethanol/acetonitrile mixtures and stirred at room temperature for about 24 hours to produce homogeneous solutions. The solutions were then cast onto silicone release paper bounded by glass rings and allowed to stand at room temperature for about 24 hours to allow solvent to evaporate. The glass rings, with polymer films attached, were transferred to a vacuum line and de-solvated, first at room temperature for about 24 hours and then at 110°C for another 24 hours. Samples were then stored in an argon-purged drybox until further study.

This work focused on PEO-based Zn(II) halide electrolytes with the general formula: $ZnX_2(PEO)_n$ where X = Cl, Br and I, and n = 4, 8, 12, 16, 20 and 24. The value

of n is the molar ratio of ether oxygens to Zn(II) ions, [O]/[Zn]. Thus, the formula, $ZnX_2(PEO)_n$, represents one mole of zinc halide for each n monomer units of PEO.

Generally, the preparation of the electrolyte films was straightforward for most of the compositions studied. However, pure ZnI_2 precipitated out of the highly concentrated composition, $ZnI_2(PEO)_4$, which restricted the study of PEO-based ZnI_2 electrolytes to compositions within the range, n = 8 to 24.

3. Experimental Procedures

Thermogravimetry (TG) was used to study the thermal stability of the samples. Measurements were performed using a DuPont 951 TGA with a DuPont 2100 controller. Samples, approximately 10 mg in weight, were heated in either dry air or nitrogen at 10°C/min.

DSC analysis was carried out in a DuPont 910 DSC cell, typically over the temperature range -110 to 200°C but higher when necessary. Samples, approximately 10 mg in weight, were hermetically sealed in aluminium pans in an argon filled drybox. They were then heated at 10°C/min (first heating), held isothermally at 200°C for 20 minutes, quenched with liquid nitrogen, and reheated from -110 to 200°C (second heating). The glass transition temperature, T_g, for all compositions studied was taken as the onset point of the transition, i.e. the point at which the extrapolated baseline intersects the extrapolated slope in the transition state.

Total ionic conductivities of PEO-based Zn(II) electrolytes were determined using ac impedance analysis with two blocking platinum electrodes. Measurements were carried out over the temperature range of 30 to 160°C and the frequency range of 10^2 to 10^5 Hz using a Solartron 1174 frequency response analyzer under computer

control. Samples were allowed to equilibrate at each temperature for 10 minutes before data collection.

Transference numbers were estimated using a combined ac/dc technique with two non-blocking zinc electrodes over the frequency range 10^{-3} to 10^{5}Hz. A 1286 Electrochemical Interface coupled with a HP computer was used to monitor the current change with time at a constant applied potential.

The chemical diffusion of ions in the Zn(II) electrolytes was measured by mapping the distribution of elements in an electrolyte couple before and after chemical diffusion had taken place. Scanning electron microscopy(SEM) and energy dispersive X-ray microanalysis (EDX) were used for the mapping. To reduce possible beam damage, all samples studied were coated with a thin layer of carbon at room temperature using vacuum sputtering. A relatively low accelerating voltage, 6 keV, was chosen for secondary electron imaging and an accelerating voltage of 18 keV was used for X-ray mapping.

Three diffusion couples were studied: (a) $ZnI_2(PEO)_{16}/PbI_2(PEO)_{16}$; (b)$PbI_2(PEO)_{16}/ZnI_2(PEO)_{16}$; and (c) $ZnBr_2(PEO)_{16}$/pure PEO. After diffusion was allowed to occur at elevated temperature under vacuum, samples were cooled to room temperature for X-ray microanalysis. Couples (a) and (b) were heated at 140°C for 18 hours and couple (c) at 70°C and 110°C, respectively, for 10 hours at each temperature.

To investigate the electrochemical reduction of Zn(II) and estimate the diffusion coefficient of Zn(II) in PEO-based Zn(II) electrolytes, the following system was studied with LiBr as the nominal supporting electrolyte: $[0.05ZnBr_2 + 0.95LiBr](PEO)_{16}$. A BAS 100A Electrochemical Analyser was used for both cyclic voltammetry (CV) and chronocoulometry (CC) analysis. A three-electrode cell was

employed using a stainless steel disk (ϕ = 5mm) as the working electrode, a zinc disk (ϕ = 1.5mm) as the reference electrode and a zinc disk (ϕ = 15mm) as the counter electrode. The working temperature was normally 100°C and the experiments were performed under vacuum or ultra-pure dry argon.

4. Results and Discussion

4.1. Thermal Stability

Pure PEO is thermally stable in an inert atmosphere until about 380°C. However, the addition of inorganic salts generally decreases the thermal stability of PEO [4]. The thermal stability of PEO-based Zn(II) electrolytes was studied in dry nitrogen by thermogravimetry (TG). The TG curves for three PEO-based Zn(II) electrolytes of concentration, n=8, are shown in Figure 1. A small weight loss of about 3 wt % or less was observed for all three samples below 100°C, the result of the evaporation of a small amount of moisture absorbed when the samples were loaded. A sharp weight loss (first-step) occurred at about 300°C, resulting from the degradation of PEO. The PEO degradation occurred at a lower temperature than with pure PEO. Most likely, the PEO stability was diminished by Zn(II) ions which, coordinating with the ether oxygens , weaken the adjacent C-O bonds (see bond 1 or 2 in Figure 2). Anion type is not a dominant factor in determining the thermal stability of these electrolytes. Similar trends were found for PEO-based zinc halide electrolytes at other concentrations.

The decomposition temperature, T_d, was defined as the temperature of maximum rate of weight loss during the first-step decomposition, and its value is plotted in Figure 3 for all PEO-based Zn(II) electrolytes studied. T_d decreases with increasing salt concentration (decreasing value of n) as would be expected.

Jones et al. [4] found that the thermal stability of pure PEO (MW=5x10^6) is very sensitive to atmosphere, as shown in Figure 4(a). The degradation of PEO occurs at a much lower temperature in dry air than in nitrogen. However, all PEO-based Zn(II) electrolytes had very similar TG behavior in either dry nitrogen or dry air, as shown in Figure 4(b).

4.2 Phase Transitions/DSC

In general, PEO-based Zn(II) halide electrolytes are highly crystalline materials at room temperature and have multi-phase structures. DSC was used to study the phase transitions in these electrolytes. Since similar DSC results were obtained regardless of whether the anion was Cl^-, Br^- or I^-, results for only $ZnBr_2(PEO)_n$ electrolytes with n = 4 to 24 are discussed in detail here.

In figure 5, DSC results for the first heating cycle are presented. Three main features can be seen. First is an endothermic peak at about 65°C, which corresponds to the melting of pure PEO and was observed for all samples, $24 \geq n \geq 8$, but not the most concentrated, n=4, for which a single endothermic peak was found at about 230°C corresponding to the melting of a crystalline PEO/salt complex with a fixed stoichiometry.

Second, a broad endothermic peak is observed above 65°C for electrolytes with compositions in the range, $20 \geq n \geq 8$. The peak temperature increased with the concentration of salt. This endothermic peak is generally believed to be associated with the existence of a PEO/salt complex. The broadness of the peak implies that the complex is poorly defined chemically. Alternatively, it may indicate that the peak is the result of the gradual dissolution of a stoichiometric phase in the PEO melt. The formation and structure of this complex phase are not well understood.

Finally, a small glass transition is observed between -20 and -30°C for all the compositions. It arises from the small fraction of amorphous phase present in the electrolytes. As is well known, the glass transition temperature, T_g, of an amorphous phase reflects the flexibility of the polymer chains in the phase. A quantitative correlation of T_g with the salt concentration present in the amorphous phase might provide insight into the nature of the ion-polymer interactions. Unfortunately, however, the salt concentration in the amorphous phase of these as-cast samples is not easily determined because of their multi-phase structures.

To obtain fully amorphous compositions, the $ZnBr_2(PEO)_n$ electrolytes were quenched from 200°C or higher to -110°C in the DSC cell after first heating cycle. DSC measurements were then carried out from -110 to 200°C. There are two main features in the DSC results on the second heating cycle, as shown in Figure 6.

First is a sharp glass transition corresponding to the fully amorphous composition, for $16 \geq n \geq 4$. Next is an exothermic peak resulting from the cold crystallization of PEO at a temperature below the melting point of pure PEO. This peak is followed by an endothermic peak corresponding to the melting of the crystalline PEO formed during the cold crystallization. These peaks should be the same size if the quenching process has succeeded in producing a sample that is, in fact, totally amorphous. This was observed to be true for the more concentrated samples. However, for the relatively dilute compositions, n=20 and n=24, some recrystallization occurred during quenching, as is indicated by the fact that the exothermic peak for cold crystallization is much larger than the endothermic peak for PEO melting.

In addition, the melting temperature of the cold crystallization phase is generally lower than 60°C for compositions of $20 \geq n \geq 4$. This result suggests that the cold

crystallization may yield a eutectic phase of PEO/salt rather than the pure PEO crystalline phase observed in the first heating cycle. Why this eutectic phase should form is not clear, but it is apparent that a constant melting phase at approximately 50°C occurs for compositions of $20 \geq n \geq 4$, which is consistent with the formation of a eutectic phase.

It was found that the glass transition temperature, T_g, for the fully amorphous compositions of all $ZnX_2(PEO)_n$ electrolytes obtained by quenching the electrolyte melts is independent of anion type, a result which indicates that it is the interaction of Zn(II) cations with the ether oxygens that principally influences the glass transition temperature of the amorphous conducting phase.

Interestingly, there is a quantitative relationship between T_g and n. A plot of T_g vs. n^{-1} is linear from $n^{-1} = 0$ for pure amorphous PEO to $n^{-1} = 0.25$ for amorphous $ZnX_2(PEO)_4$, as shown in Figure 7. The numerical relationship that results is shown in Eqn. 1.

$$T_g\,(°C) = -62 + 403\,\frac{[Zn]}{[O]} \qquad (1)$$

Eqn. 1 is very useful in predicting the salt concentration in an amorphous phase with a known T_g. Unfortunately it may not be applied to an electrolyte with only a small fraction of amorphous phase, e.g. the amorphous phase in as-cast PEO electrolytes at room temperature, because the co-existing crystalline phase may influence the T_g of the adjacent amorphous phase.

Finally, it is worthwhile to emphasize that the higher the salt concentration in the amorphous phase, the higher the T_g, an effect, in general, the result of strong cation-polymer and possibly cation-anion interactions. If a cation can interact simultaneously with ether oxygens in one or more polymer chains, transient inter- or intra-crosslinks may be formed, as pointed out by Vincent [5]. These crosslinks

will have a first-order effect on the segmental motion of the polymer chains, and T_g will increase. If a strong cation-anion interaction occurs, the crosslink center could also involve anions, which would act as temporary bridges between pairs of cations solvated by nearby polymer chains. For the PEO-based Zn(II) halide electrolytes studied here, no anion effect on T_g was observed, a result which suggests that the dominant inter- and intra-chain links are formed by cations.

Previous work by Ueberreiter and Kanig [6] bears on the relationship of crosslink density and T_g. In 1950 they pointed out that the change in glass transition temperature with increasing crosslink density, ΔT_g, is proportional to the cross-link density, D, as in Eqn. 2:

$$\Delta T_g = ZD \qquad (2)$$

where Z is a constant. This relationship has recently been verified by Glans et al. [7] using crosslinked polystyrene. Interestingly, eqn. 1, obtained in this work, can be rearranged into eqn. 3

$$\Delta T_g = 403 \frac{[Zn]}{[O]} \qquad (3)$$

where $\Delta T_g = T_{g\,(PEO/ZnX_2)} - T_{g\,(PEO)}$. This relationship clearly indicates that Zn(II) cations can effectively interact with ether oxygens on the PEO chains to produce inter- or intrachain crosslinks.

4.3 Conductivity

Conductivity measurements were carried out on a series of PEO-based zinc halide electrolytes with different salt concentrations. The variation of conductivity with temperature and total salt concentration is discussed in this section. However, it is useful first to review selected DSC results for related PEO-based Zn(II) halide electrolytes.

Shown in Figure 8 are the DSC curves for $ZnCl_2(PEO)_{24}$, $ZnBr_2(PEO)_{20}$, $ZnI_2(PEO)_{20}$, and $ZnCl_2(PEO)_4$ electrolytes. The former three electrolytes contained a large fraction of pure PEO crystalline phase, which gives rise to the sharp endothermic peak at about 65°C, as well as PEO/salt complex phases which melted over the broad temperature range of 75°C to 175°C. However, the latter composition, $ZnCl_2(PEO)_4$, contained no pure PEO, but rather a fixed stoichiometric PEO/salt complex phase which melted at about 190°C

Figure 9 presents the temperature-dependence of the conductivity for the most highly conducting compositions for each anion, $ZnCl_2(PEO)_{24}$, $ZnBr_2(PEO)_{20}$ and $ZnI_2(PEO)_{20}$, together with the result for $ZnCl_2(PEO)_4$ for comparison. Of these three Zn(II) halide electrolytes, the bromide and iodide compositions had similar conductivities over the entire temperature range studied (30 to 160°C), whereas $ZnCl_2(PEO)_{24}$ had significantly lower conductivity. The main feature observed for these electrolytes was a sudden change of conductivity at about 60°C, at which the pure PEO crystalline phase started to melt. At temperatures above 60°C, Arrhenius-type conductivity behavior was observed for all three electrolytes. The conductivity of the $ZnCl_2(PEO)_4$ electrolyte followed Arrhenius-type behavior over the entire temperature range studied.

Clearly, the melting of the pure PEO phase at around 65°C is responsible for the sudden conductivity increase observed for the electrolytes containing crystalline PEO. PEO melting results in the formation of an amorphous conducting phase with a lower salt concentration, thus increasing the local mobility of the polymer chains. Thus, a dramatic increase in the mobility of the charge carriers is presumably responsible for the sudden increase of conductivity at the PEO melting temperature.

Looking back to the DSC curves in Figure 8 for the three Zn(II) halide electrolytes

with $24 \geq n \geq 20$, the existence of PEO/salt complex phases was observed, all of which melted over a broad temperature range between 75°C and 175°C. Clearly, the melting or dissolution of the PEO/salt complex phases releases more salt into the amorphous conducting electrolyte, and, therefore, generates more charge carriers. However, the corresponding temperature dependence of conductivity in Figure 9 shows no clear transition at temperatures above 65°C, indicating that the thermal activation of mobility is the principal factor influencing the conductivity, not charge carrier concentration.

Finally, the compositional dependence of conductivity for PEO-based Zn(II) electrolytes is shown in Figure 10. The highest conductivity occurs at a relatively dilute composition for all three halide electrolytes. Currently, there is no satisfactory explanation for the conductivity/concentration relationship. Both the number of charge carriers and their mobilities are likely to be concentration dependent in a rather complicated manner.

4.4 Mobility of Zn(II) Species

Three approaches were employed to study the mobility of Zn(II) species in the PEO-based electrolytes: (i) measurement of the Zn(II) transference number using ac and dc electrochemical techniques; (ii) qualitative investigation of Zn(II) diffusion using SEM/EDX; and (iii) quantitative determination of the Zn(II) diffusion coefficient using cyclic voltammetry and chronocoulometry, CV/CC.

It is worth noting that PEO is only effective at solvating cations. Cation solvation occurs by the electrostatic interaction between a cation and the negative (oxygen) end of the polymer dipole or by the partial sharing of a lone pair of electrons on the ether oxygen, leading to the formation of a coordinate bond. Thus, PEO has only a

limited ability to shield ionic charges from each other, which gives rise to ion pairing and ion cluster formation due to the Coulombic interaction between cations and anions, as has been described in several earlier studies [8,9]. Ion-ion interactions are also encouraged by the fact that the PEO-based electrolytes studied are in conventional terms very concentrated solutions. For example, the molar concentration of a $ZnBr_2(PEO)_{20}$ electrolyte is about 1M, assuming the average electrolyte density is about that of PEO, 1.2 g/cm^3.

In a PEO-based $ZnBr_2$ electrolyte, the possible charged species include free Br(-I) ions, neutral ($ZnBr_2$) species, negatively charged (ZnBr)(-I)pairs, as well as Zn(II) ions associated with ether oxygens in the polymer chains. The mobility of Zn(II) could involve the motion of two populations of charged Zn(II) carriers: one that is associated with the ether oxygens and the another associated with anions alone. As discussed in earlier sections, both TG and DSC results have indicated strong interactions between Zn(II) cations and the ether oxygens in the PEO chains. It is, therefore, possible that one population of Zn(II) ions is trapped by the polymer and the other moves as complex ion clusters.

4.4.1 AC and DC polarization measurements

Complex ac analysis and dc polarization measurements were performed on a series of PEO-based Zn(II) halide electrolytes, $ZnX_2(PEO)_n$, where X = Cl, Br and I and n = 16 to 24 at 100°C. As an example of the results, Figure 11 shows an ac impedance spectrum for a $Zn/ZnBr_2(PEO)_{16}/Zn$ electrochemical cell. The diffusion impedance, $Z_d(0)$, is about two orders magnitude higher than the bulk resistance, so the transference number of Zn(II), as calculated from Eqn.4, is very low.

$$\tau_+ = \frac{R_b}{R_b + Z_d(0)} \sim 0.01 \qquad (4)$$

A dc measurement was also carried out in which an identical cell was polarized at a constant potential of 20mV. The current decayed rapidly to a very low level, as shown in Figure 12, and the transference number estimated from this measurement is again on the order of 0.01. This measurement was repeated many times, and the results were consistent.

However, as can be seen in Figure 11, the interfacial resistance, R_e, is about two orders magnitude higher than the bulk resistance of the electrolyte, which is certainly far from the ideal non-blocking electrode/electrolyte interface. This observation suggests that Zn(II) species, in fact, may be highly mobile in the electrolytes, but their mobility may be masked by the high interfacial impedance at the electrode/electrolyte interface. The results also raise the question of whether high interfacial impedance is a particular characteristic of this electrochemical couple or a more general property of the interfaces between electrodes and polymer electrolytes. Relatively little is known about electrokinetics at high molecular weight polymer electrolyte interfaces, but it might be expected that, if the electroactive ions are transported through the motion of complex ion clusters, charge transfer kinetics might well be slow.

4.4.2 Chemical diffusion of Zn(II) species

Because of the ambiguities introduced into the electrochemical measurements by the extremely high interfacial resistance, experiments using scanning electron microscopy coupled with energy dispersive X-ray microanalysis, SEM/EDX, were designed to investigate the chemical diffusion of Zn(II) species. In brief, two polymer electrolyte films, each containing different salt concentrations, were pressed against each other at room temperature to form a diffusion couple. The sandwich

was then heated at a fixed temperature to allow whatever species were mobile to diffuse. SEM/EDX was used to map the cation and/or anion distributions before and after the diffusion.

To examine whether or not Zn(II) species are mobile in PEO-based electrolytes, it was useful to pair Zn(II) electrolytes with other PEO-based electrolytes in which cations are known to move. Previous studies by Huq at el. [10] have shown that, in PEO-based PbI_2 electrolytes, Pb(II) is mobile and has a transference number of about 0.6 at 140°C. So, a bi-layer diffusion couple of the type, $PbI_2(PEO)_{16}/ZnI_2(PEO)_{16}$, was constructed and studied first. A salt concentration of n=16 was chosen as a compromise among the following requirements: (i) high conductivity, which usually occurs at relatively dilute electrolyte systems; and (ii) sufficient concentration of Zn(II) species for EDX analysis. In addition, to focus the issue on the diffusion of cations, the same anion was chosen for both electrolytes and the same stoichiometric concentration.

Shown in Figure 13 are the maps of Pb(II) and Zn(II) before and after the diffusion couple was heated at 140°C. Both Pb(II) and Zn(II) diffused. Since this particular couple consisted of a layer of $PbI_2(PEO)_{16}$ on top of $ZnI_2(PEO)_{16}$, most of the diffusion of Zn(II) occurred only within the thickness of the Pb(II) film. Another diffusion couple $ZnI_2(PEO)_{16}$ /$PbI_2(PEO)_{16}$ was formed by placing a smaller square of the Zn(II) sample in the center of a large square of the Pb(II) electrolyte. Again (Fig. 14), significant diffusion of Zn(II) was observed, not only through the thickness of the films but also along their length and width. These results indicate clearly that Zn(II) is mobile in some form in PEO-based ZnI_2 electrolytes.

Finally, the diffusion of both Zn(II) and Br(-I) in pure PEO was investigated in a diffusion couple formed of $ZnBr_2(PEO)_{16}$ and pure PEO. The results again indicate

that both Zn(II) and Br(-I) species were mobile. Even upon heating at 70°C for ten hours, both Zn(II) and Br(-I) were observed to diffuse, as shown in Figure 15.

It should be pointed out that one of the disadvantages of using SEM/EDX to investigate diffusion in the PEO-based electrolytes is that it cannot differentiate between charged and neutral mobile species, because the analysis is based solely on the characteristic X-rays of the elements involved. However, this work clearly demonstrates that some Zn(II) species are mobile in PEO-based Zn(II) halide electrolytes, although the results were not of sufficient quality to estimate the diffusion coefficient of the species involved.

4.4.3 Diffusion coefficient of Zn(II) species

Chronocoulometry (CC) coupled with cyclic voltammetry (CV) was used to measure the diffusion coefficient of Zn(II) species in a $[0.05ZnBr_2+0.95LiBr](PEO)_{16}$ electrolyte. LiBr was introduced in the hope that it would function as a supporting electrolyte and minimize the effective of Zn(II) migration. A three-electrode electrochemical cell was designed for both CV and CC studies. The cell consisted of a stainless steel disk as working electrode (WE), a counter, or auxiliary electrode (CE) made of a disk of pure zinc foil, and a small pure zinc reference electrode (RE).

The electrochemical reactions of an electrolyte containing only the pure supporting electrolyte, $LiBr(PEO)_{16}$, were studied at 100°C to determine the potential window within which a diffusion controlled electrochemical process could be expected in a Zn(II) electrolyte. The stability window was found to be -1.0V to +2.0V vs. a Ag/AgBr reference electrode at a scan rate of 20 mV/S.

The following electrochemical cell was used to study the electrochemical characteristics of a Zn(II) electrolyte.

SS vs. Zn / $[0.05ZnBr_2+0.95LiBr](PEO)_{16}$ / Zn

Cyclic voltammograms were recorded for the cell at different scan rates and temperatures. Starting at the rest potential for each CV, the potential was first scanned in the negative direction and then reversed to the positive direction. The potential range was -1.0V to +1.0V vs. the reference electrode.

A typical cyclic voltammogram recorded at a scan rate of 20 mV/S for a sample at 100°C shows a pair of oxidation/reduction processes, as in Figure 16(a). The reduction peak at about -0.35V is presumably due to the reduction of Zn(II) to Zn, and the oxidation peak at +0.35V is the result of the reverse reaction. The charge transfer kinetics in this system appear to be slow. The peaks were quite reproducible, after an initial cycle in which the working electrode was conditioned. The scan rate dependence of the cyclic voltammograms at 100°C is shown in Figure 16(b). A second oxidation peak was observed around 0.60V at scan rates, $v \geq$ 50mV/S, but no corresponding reduction peak. The temperature dependence of the cyclic voltammograms at a scan rate of 20mV/S is summarized in Figure 16(c).

In summary, CV results indicate that the charge transfer process is rather slow at a SS/$[0.05ZnBr_2+0.95LiBr](PEO)_{16}$ interface. Although what appears to be a Zn(II)/Zn reduction/oxidation was observed at low scan rates, $v \leq$ 20mV, and 100°C, the oxidation process became more complex at higher scan rates and lower temperatures. It is worth noting that the measured peak potential may shift as the result of the IR drop which can only be partially compensated in most cases. It must be pointed out that the potentials reported here were measured only with respect to a pseudo-reference electrode and thus are not thermodynamically significant.

In an attempt to measure the diffusion coefficient of Zn(II), double-step chronocoulometry was performed on the cell:

SS vs. Zn / $[0.05ZnBr_2+0.95LiBr](PEO)_{16}$ / Zn

at 100°C. The initial potential was chosen as the rest potential of the cell. The step potentials were -350mV for the reduction and +350mV for the oxidation. Although a double-step CC experiment was performed, the focus in this work was on the reduction process rather than the oxidation process which CV studies indicate is somewhat complex. An apparently linear relationship of Q vs. $t^{1/2}$ was observed for the reduction process over a 500mS pulse.

Ideally, the current-time response of an electrochemical process under diffusion control follows the Cottrell equation:

$$i(t) = i_d(t) = \frac{nFA D_o^{1/2} C_o^{\infty}}{\pi^{1/2}} t^{-1/2} \qquad (5)$$

Integration of Eqn. 5 shows that Q should vary linearly with $t^{1/2}$ according to the expression:

$$Q = \frac{2nFAD_o^{1/2} C_o^{\infty}}{\pi^{1/2}} t^{1/2} \qquad (6)$$

Although a linear relationship of Q vs. $t^{1/2}$ was observed at -350mV, the slope of a similar plot of data taken at -400mV increased. To verify this observation, a series of CC measurements were carried out at increasingly negative step potentials of -450, -500, -600, -650, -700, -750, -800, and -850mV. The electrochemical cell was allowed to rest for at least 6 hours in between each measurement to permit initial conditions to be re-established. When the slope of Q vs $t^{1/2}$ was plotted against the applied step potential, a monotonic increase of the slope with the applied step potential was observed, as shown in Figure 17. This result suggests that the reduction of Zn(II) species in the cell is not controlled simply by diffusion but also by migration, despite the presence of a large quantity of the "supporting" electrolyte (95 mol% of LiBr).

The question then arose of how to eliminate the migrational effect, which appeared to dominate mass transport in this PEO-based Zn(II) solid electrolyte composition. The answer is not simple. Further studies showed that the Zn(II) electrolyte containing LiBr, $[0.05ZnBr_2+0.95LiBr](PEO)_{16}$, has an unusually high conductivity, higher than that of either pure salt electrolyte, $ZnBr_2(PEO)_{16}$ or $LiBr(PEO)_{16}$. This result suggests that LiBr does not behave as a supporting electrolyte at all; rather, it may form complex species with zinc ions, resulting a fundamental change in the species in the electrolyte system. As a consequence, a systematic study of the mixed-salt effect in PEO-based electrolytes was conducted, and the results are reported in a separate paper [11].

5. Conclusions

PEO-based Zn(II) halide electrolytes are complex mixtures, generally of three phases: a pure PEO crystalline phase which melts about 65°C and a PEO/salt complex phase characterized by a broad endothermic DSC peak above 65°C, both embedded in an amorphous ionically conductive polymer/salt solution. The fraction of each component present depends on a number of factors, including salt type, concentration, temperature, and thermal history. For example, as the temperature is decreased, the fraction of crystalline components increases, and in highly concentrated compositions, such as $ZnCl_2(PEO)_4$ or $ZnBr_2(PEO)_4$, no crystalline PEO phase is observed, rather a fixed stoichiometric PEO/salt complex exists together with a small fraction of an amorphous phase.

By, quenching Zn(II) electrolyte melts from 200 to -100°C, the glass transition temperature, T_g, of the fully amorphous compositions can be obtained. This work has demonstrated that T_g increases linearly with the mole ratio of $\frac{[Zn]}{[O]} = n^{-1}$:

$$T_g\,(°C) = -62 + 403\,\frac{[Zn]}{[O]}$$

from $n^{-1} = 0$ (pure PEO) up to $n^{-1} = 0.25$ ($ZnX_2(PEO)_4$ with X = Cl and Br). In addition, T_g is independent of the anion type: Cl(-I), Br(-I) or I(-I). These results clearly show that Zn(II) cations interact with ether oxygens in the PEO chains to form inter- and/or intrachain crosslinks.

The conductivity of PEO-based Zn(II) halide electrolytes has been studied as a function of temperature (30 to 160°C) and salt concentration (n = 4 to 24). Certain compositions, n=24 for X = Cl(-I), and n=20 for X = Br(-I) or I(-I), have rather high conductivities compared to other PEO-based divalent cation electrolytes. It appears that the conductivity is primarily determined by the segmental mobility of the PEO chains, and, therefore, the mobility of the charge carriers in the amorphous conducting phase.

Chemical diffusion studies using SEM/EDX have clearly demonstrated that Zn(II) species are mobile in PEO-based Zn(II) halide electrolytes. Attempts to measure the transference number of Zn(II) by both ac and dc polarization proved to be difficult, as a result of an unusually high interfacial impedance observed at a Zn/Zn(II) electrolyte interface.

It is important to point out that all the electrolytes studied in this work are, in conventional terms, very concentrated solutions. In an immobile solvent with as low dielectric constant as PEO, it is inevitable that large populations of ion pairs and ion clusters will form in the amorphous conducting phase. The present work suggests that there may be two populations of Zn(II) species in PEO-based Zn(II) halide electrolytes, one associated with the ether oxygens and another associated with the anions. Since both TG and DSC results indicate a rather strong interaction

between Zn(II) cations and the ether oxygens in the PEO chains, it is likely that Zn(II) associated with PEO is considerably less mobile than that associated with the anions.

6. Acknowledgements

This work was supported by a grant from the Defense Advanced Research Projects Agency through a contract monitored by the Office of Naval Research. Additional support from the NSF-MRL program under grant no. DMR88-19885 is gratefully acknowledged.

References

[1] *Polymer Electrolyte Reviews-1*, J. R. MacCallum and C. A. Vincent, eds., Elservier Applied Science, 1987.

[2] *Polymer Electrolyte Reviews-2*, J. R. MacCallum and C. A. Vincent, eds., Elservier Applied Science, 1989.

[3] G, C. Farrington and R. G. Linford, in *Polymer Electrolyte Reviews-2*, J. R. MacCallum and C. A. Vincent, eds., Elservier Applied Science, 1989.

[4] G. K. Jones, A. R. McGhie, and G. C. Farrington, to be appeared in *Macromolecules*.

[5] C. A. Vincent, in *Electrochemical Science and Technology of Polymer-2*, Elsevier Applied Science, R. G. Linford ed., 1990.

[6] K. Ueberreiter, and G. Kanig, *J. Chem. Phys.*, **18** (1950) 399.

[7] J. H. Glans, and D. T. Turner, *Polymer*, **22** (1981) 1540.

[8] B. L. Papke, M. A. Ratner, and D. F. Shriver, *Solid State Ionics*, **5** (1981) 685.

[9] R. Dupon, B. L. Papke, M. A. Ratner, D. H. Whitmore, and D. F. Shriver, *J. Am. Chem. Soc.* **104** (1982) 6247.

[10] R. Huq, and G. C. Farrington, *J. Electrochem. Soc.*, **135** (1988) 524.

[11] H. Yang, and G. C. Farrington, submitted to J. of Poly. Sci., Part B, 1991

Figure Captions

Figure 1 TG curves of $ZnX_2(PEO)_8$ with X = Cl, Br and I in dry N_2

Figure 2 Proposed degradation mechanism in PEO-based electrolytes

Figure 3 Decomposition temperature, T_d, of $ZnX_2(PEO)_n$ in dry N_2

Figure 4 TG curves in both dry N_2 and air for (a) pure PEO with MW=$5x10^6$; and (b) $ZnBr_2(PEO)_{16}$

Figure 5 DSC curves for $ZnBr_2(PEO)_n$ electrolytes at first heating cycle

Figure 6 DSC curves for $ZnBr_2(PEO)_n$ electrolytes at second heating cycle

Figure 7 Glass transition temperature of the fully amorphous $ZnX_2(PEO)_n$ electrolytes

Figure 8 DSC curves of $ZnCl_2(PEO)_{24}$, $ZnBr_2(PEO)_{20}$, $ZnI_2(PEO)_{20}$, and $ZnCl_2(PEO)_4$ electrolytes

Figure 9 Temperature-dependence of conductivity of PEO-based Zn(II) electrolytes

Figure 10 Composition-dependence of conductivity at various temperatures for (a) $ZnCl_2(PEO)_n$, (b) $ZnBr_2(PEO)_n$, and (c) $ZnI_2(PEO)_n$

Figure 11 AC impedance spectra for Zn / $ZnBr_2(PEO)_{16}$ / Zn at 100°C with f = 10^{-3} - 10^6Hz

Figure 12 DC polarization measurement for Zn / $ZnBr_2(PEO)_{16}$ / Zn at 100°C with V = 20mV

Figure 13 EDX maps of Pb(II) and Zn(II) before and after diffusion in $PbI_2(PEO)_{16}$ / $ZnI_2(PEO)_{16}$ diffusion couple

Figure 14 EDX maps Zn(II) before and after diffusion in $ZnI_2(PEO)_{16}$/$PbI_2(PEO)_{16}$ diffusion couple

Figure 15 EDX maps Zn(II) before and after diffusion in $ZnBr_2$/pure PEO diffusion couple

Figure 16 Cyclic voltammograms of $[0.05ZnBr_2+0.95LiBr](PEO)_{16}$ at 100°C:
(a) with a scan rate of 20mV/S (E vs. Zn);
(b) with various scan rates; and
(c) with a scan rate of 20mV/S at various temperatures

Figure 17 Dependence of the slope of Q vs. $t^{1/2}$ on the applied step potential at 100°C

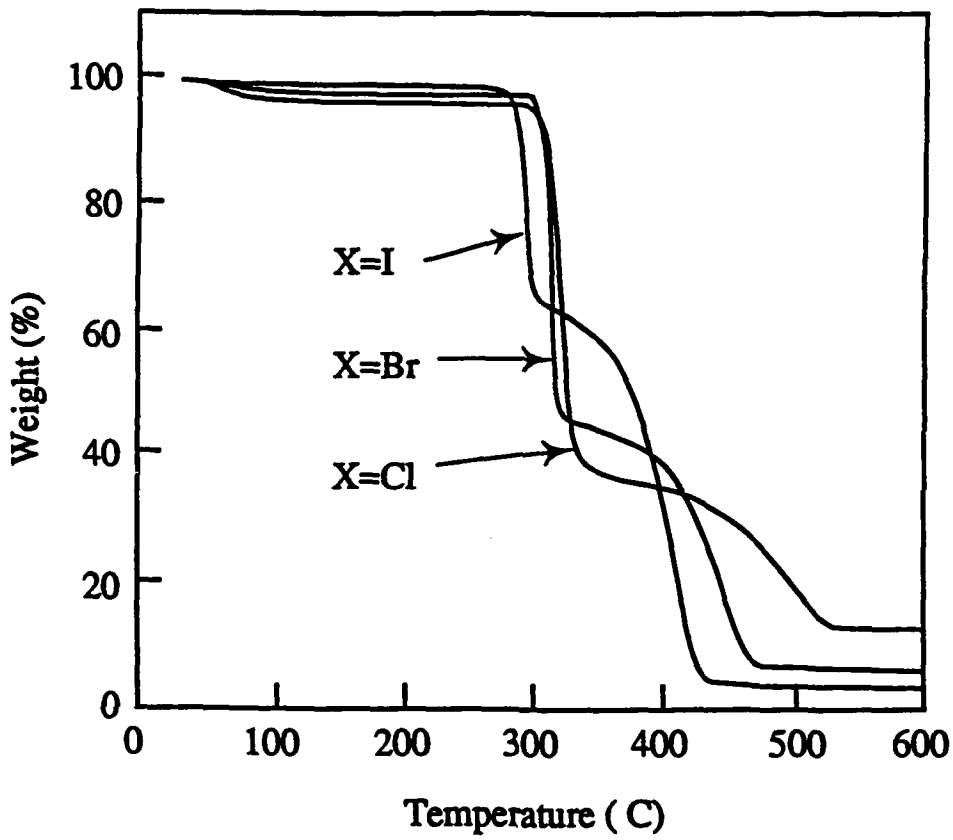

Figure 1 TG curves of $ZnX_2(PEO)_8$, where X=Cl, Br, and I in dry N_2

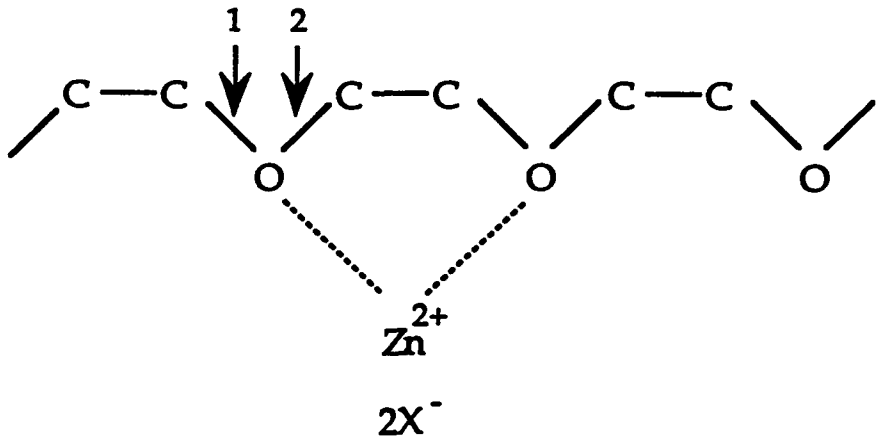

Figure 2 Proposed degradation mechanism in PEO-based electrolytes

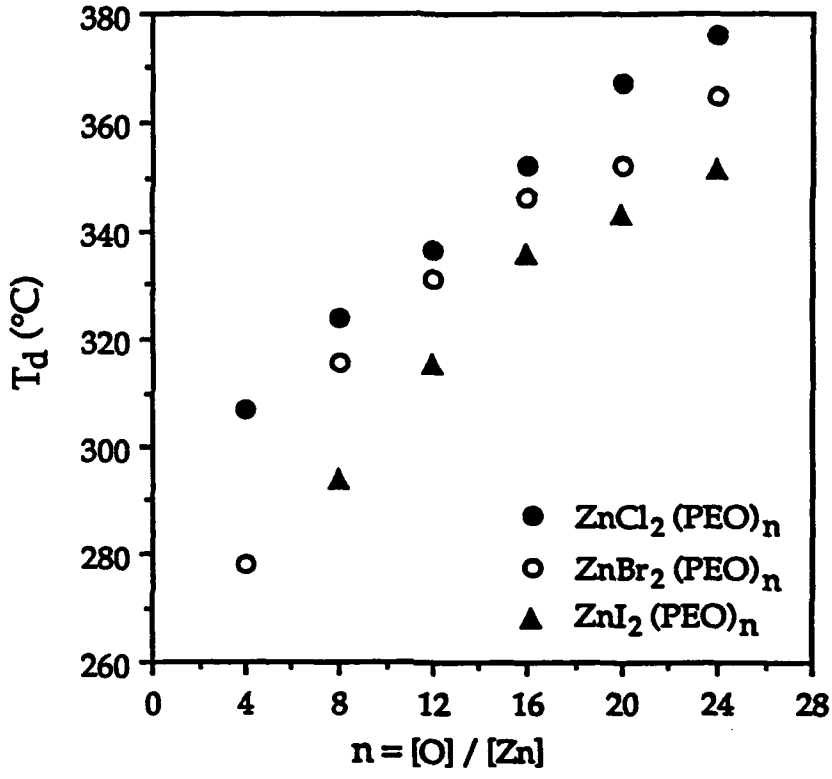

Figure 3 Decomposition temperature, T_d, of $ZnX_2(PEO)_n$ in dry N_2

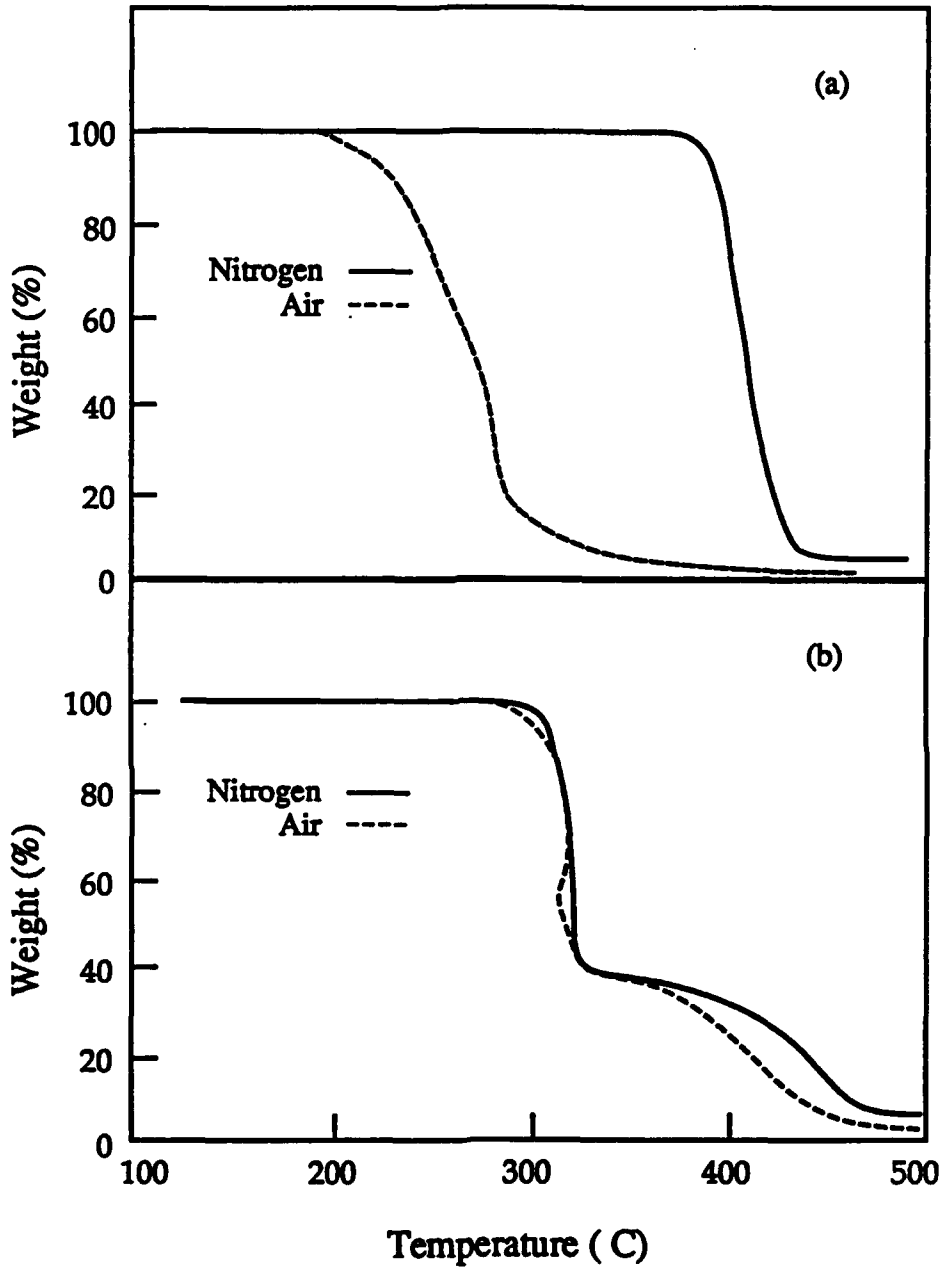

Figure 4 TG curves in both dry N_2 and air for (a) pure PEO with MW=$5x10^6$; and (b) $ZnBr_2(PEO)_{16}$

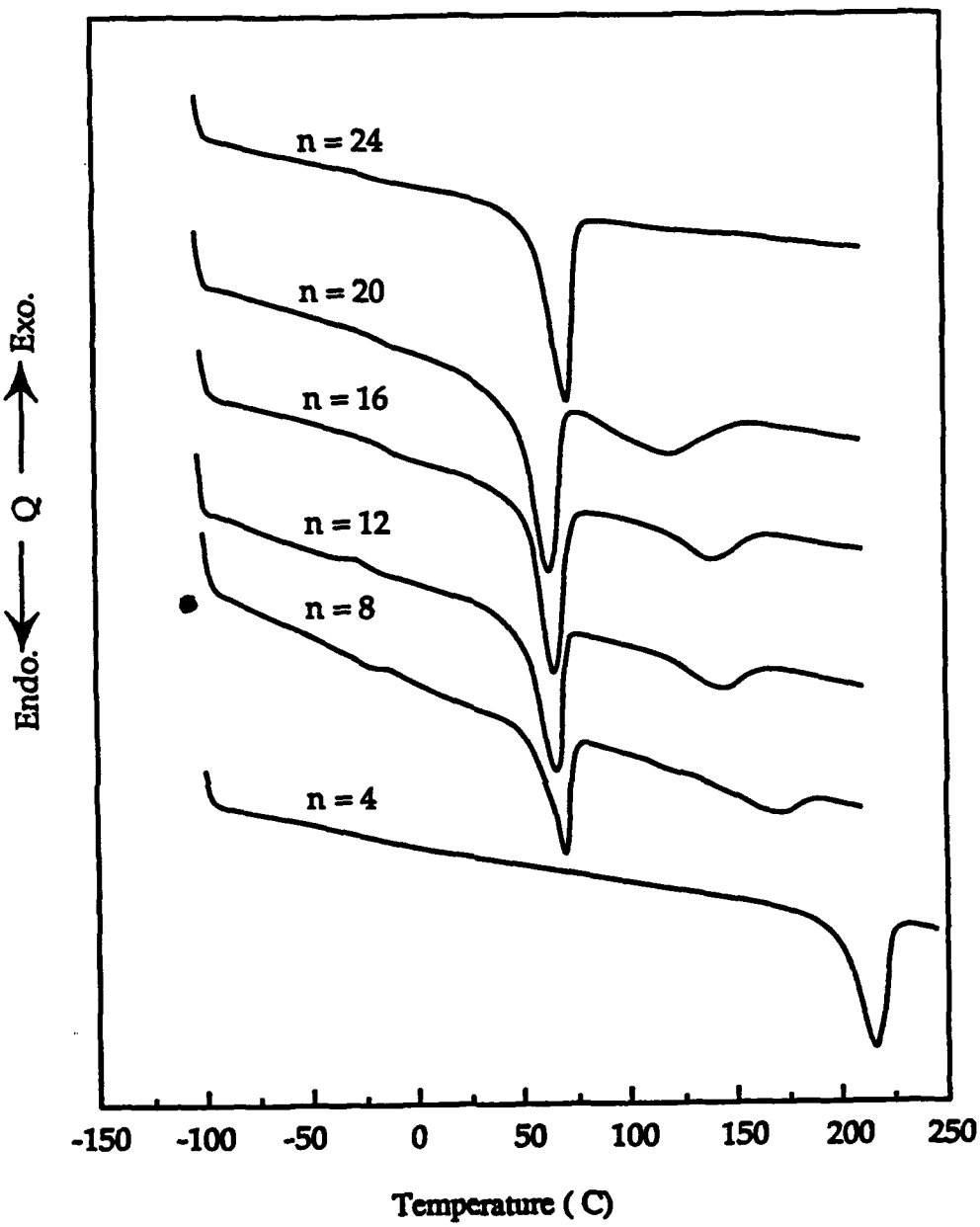

Figure 5 DSC curves for $ZnBr_2(PEO)_n$ electrolytes at first heating cycle

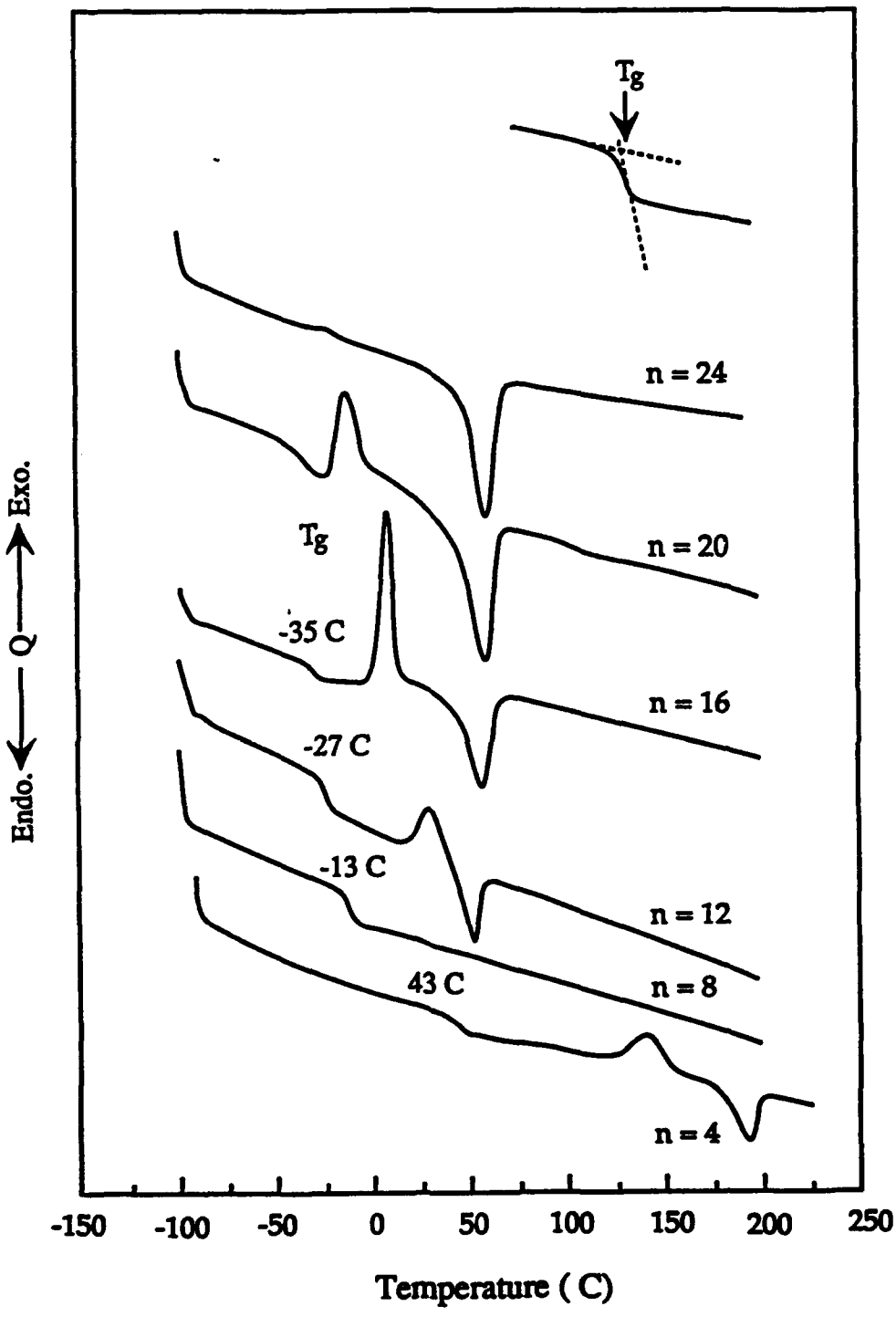

Figure 6 DSC curves for $ZnBr_2(PEO)_n$ electrolytes at second heating cycle

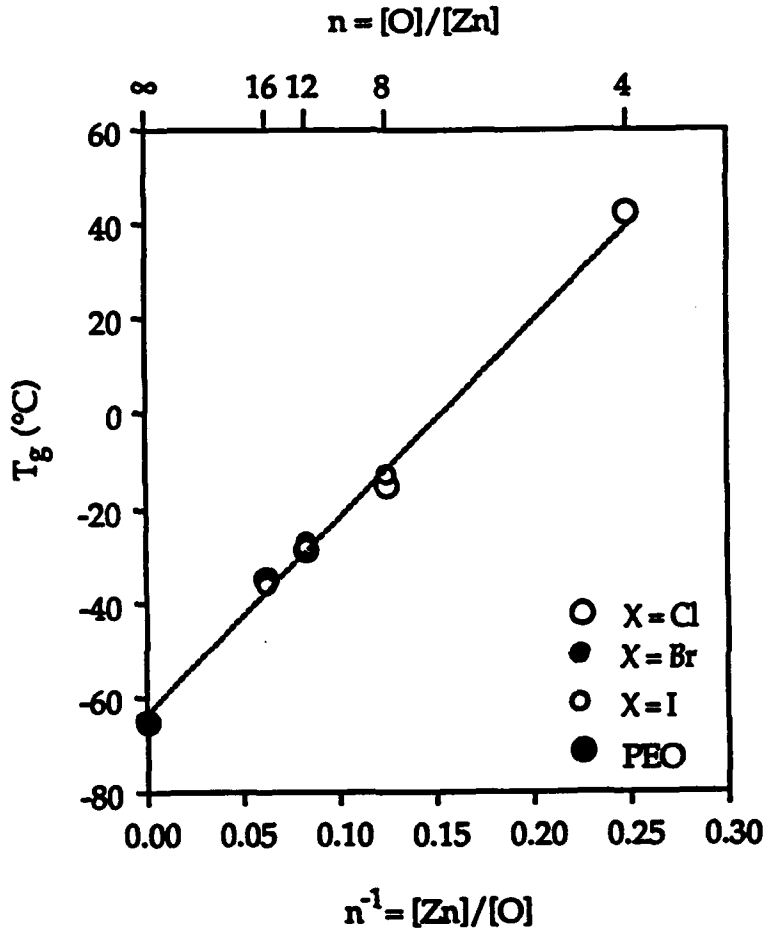

Figure 7 Glass transition temperatures of the fully amorphous $ZnX_2(PEO)_n$ electrolytes

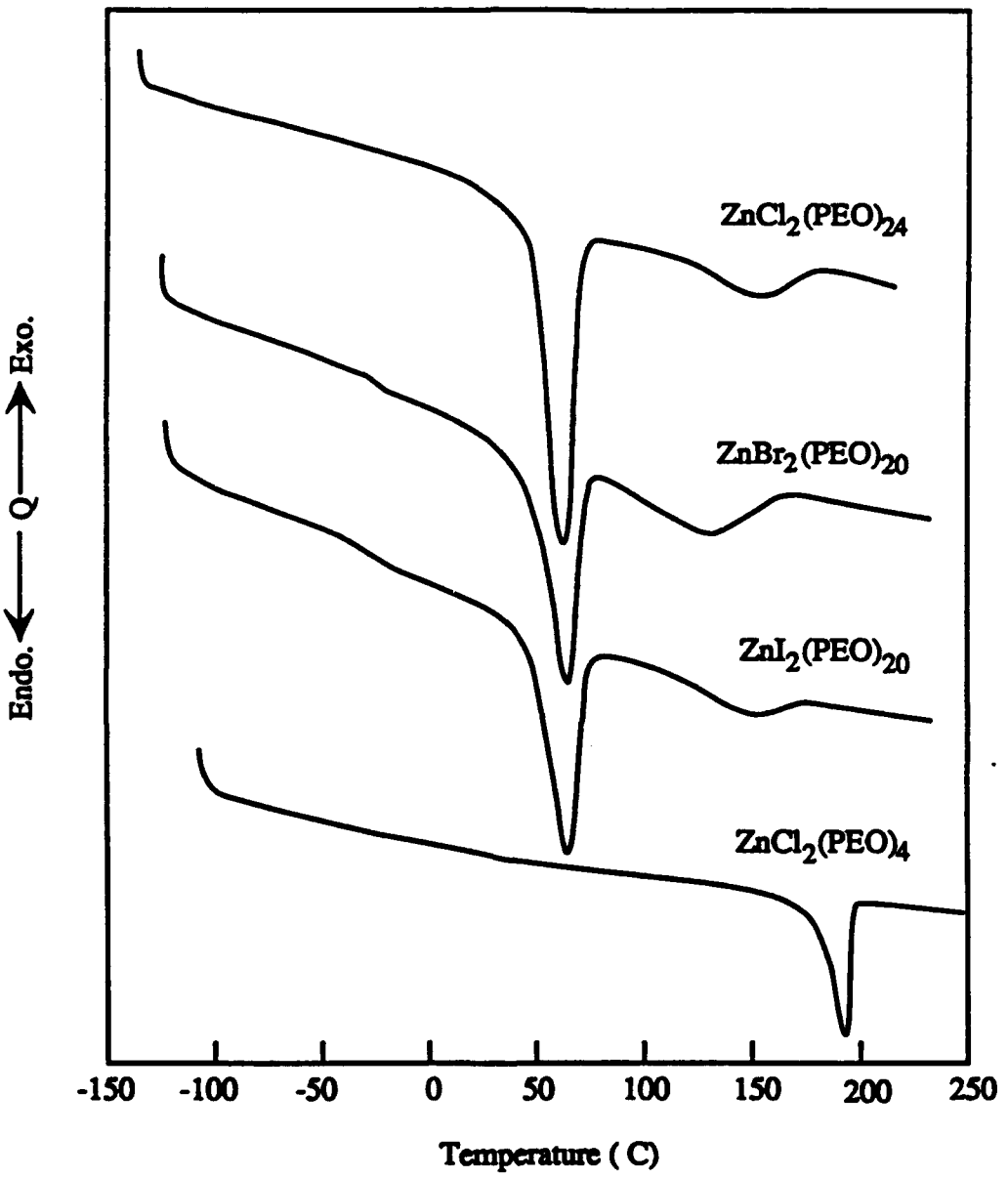

Figure 8 DSC curves of PEO-based Zn(II) halide electrolytes

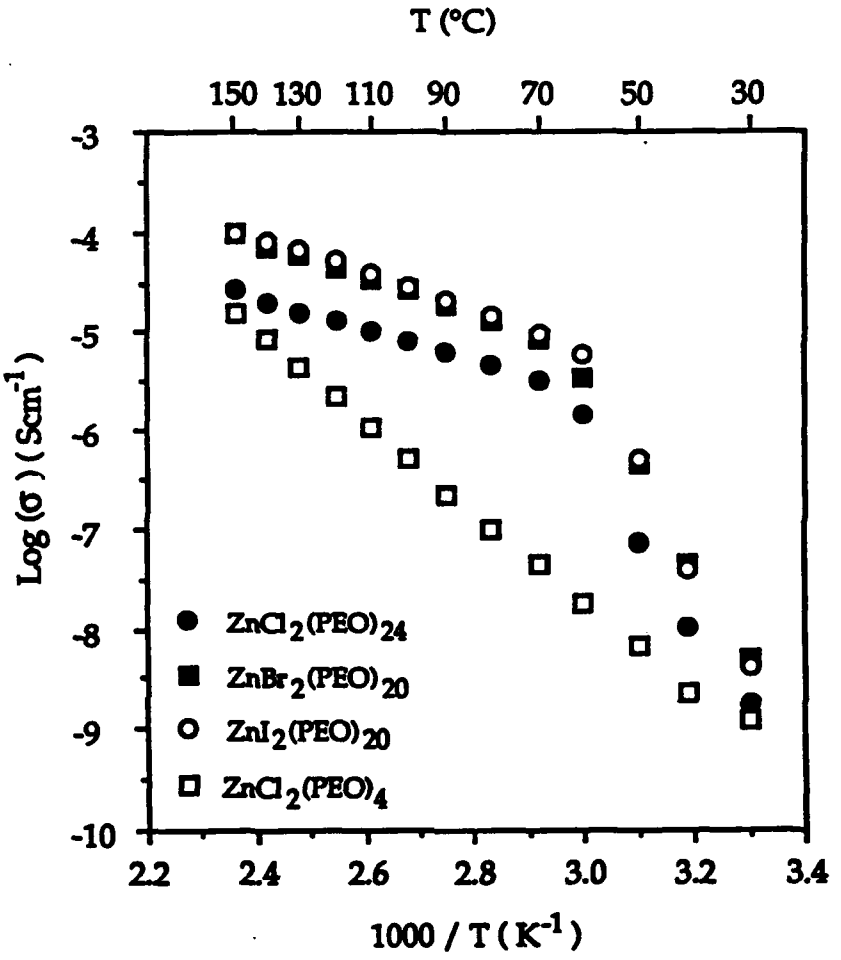

Figure 9 Temperature-dependence of conductivity of PEO-based Zn(II) Electrolytes

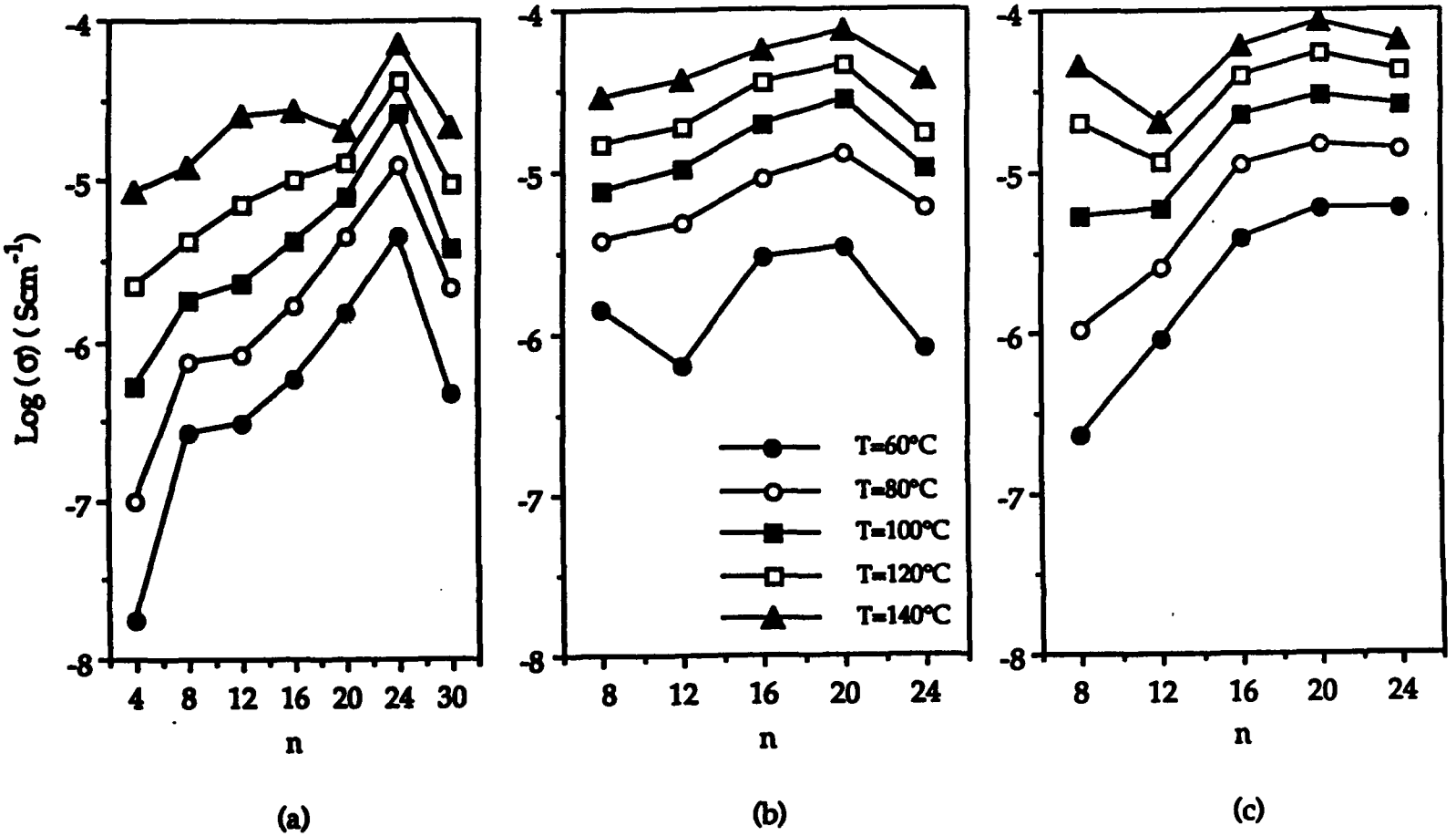

Figure 10 Composition-dependence of conductivify at various temperatures for (a) $ZnCl_2(PEO)_n$, (b)$ZnBr_2(PEO)_n$, and (c) $ZnI_2(PEO)_n$

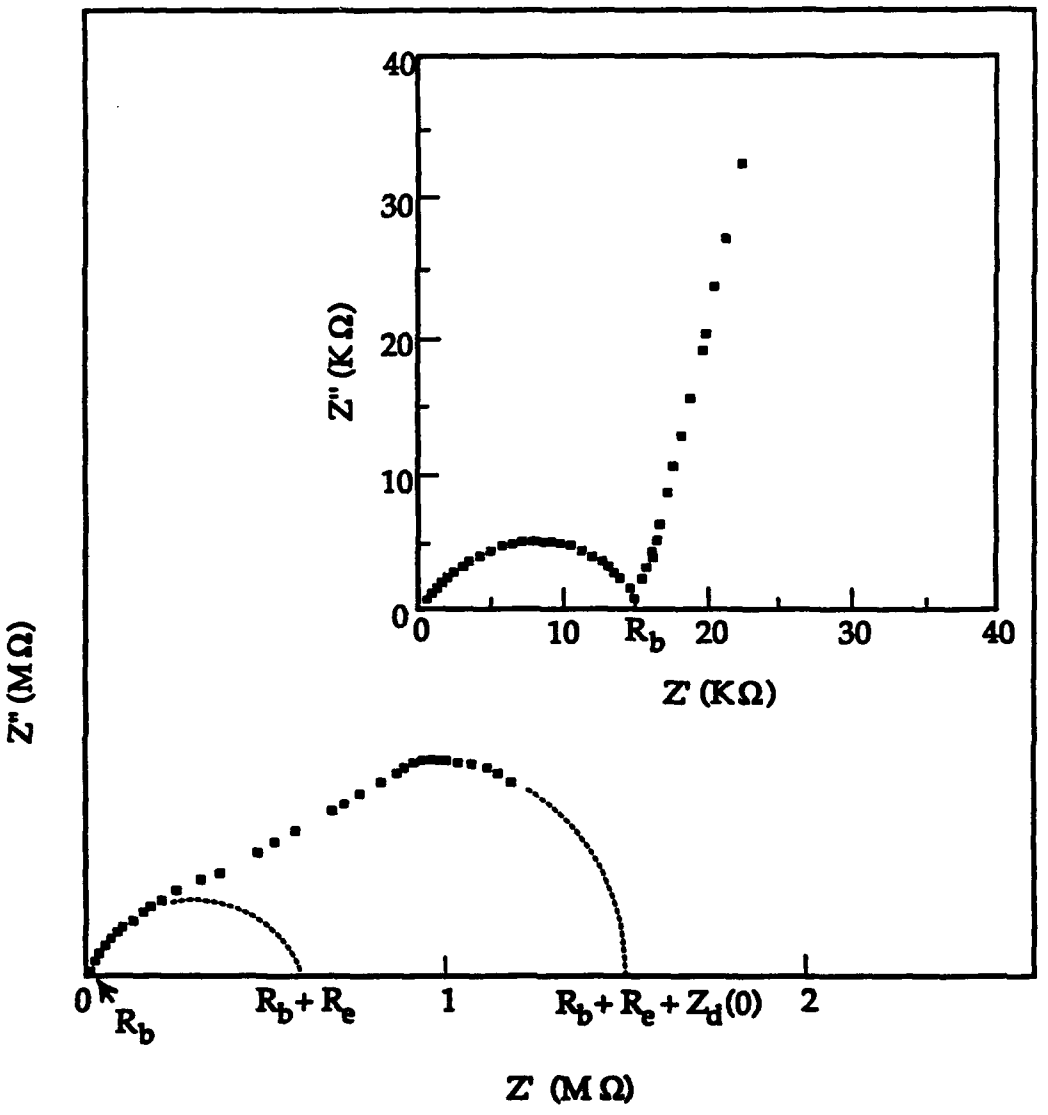

Figure 11 AC impedance spectra for $Zn/ZnBr_2(PEO)_{16}/Zn$ at 100°C with $f = 10^{-3} - 10^{6}$Hz

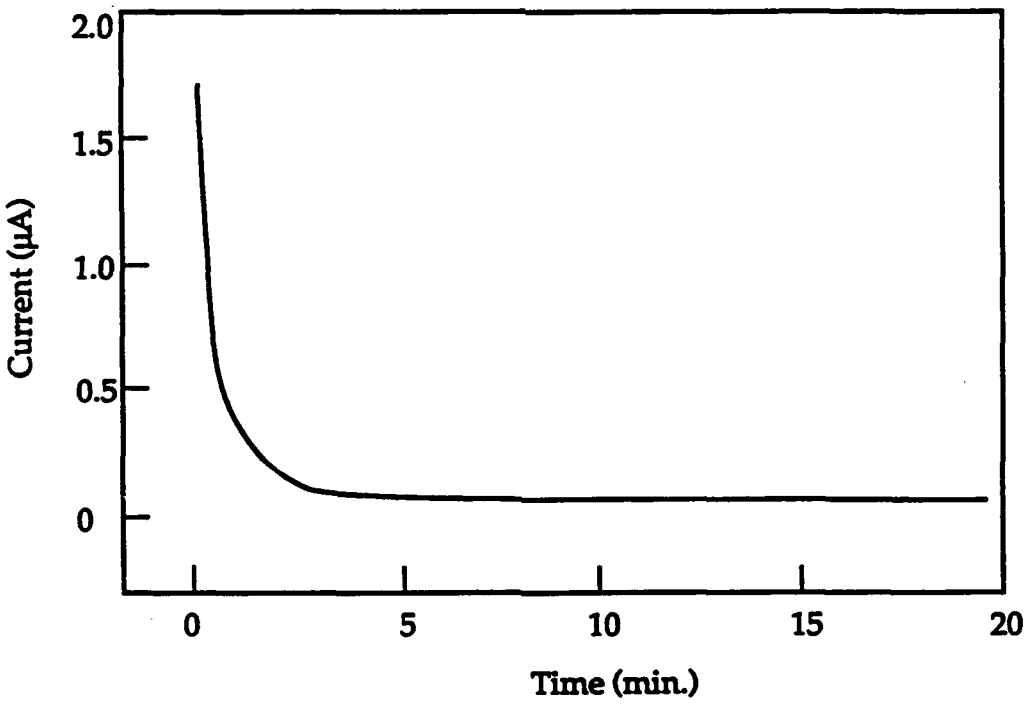

Figure 12 DC polarization measurement for $Zn/ZnBr_2(PEO)_{16}/Zn$ at 100°C with V= 20mV

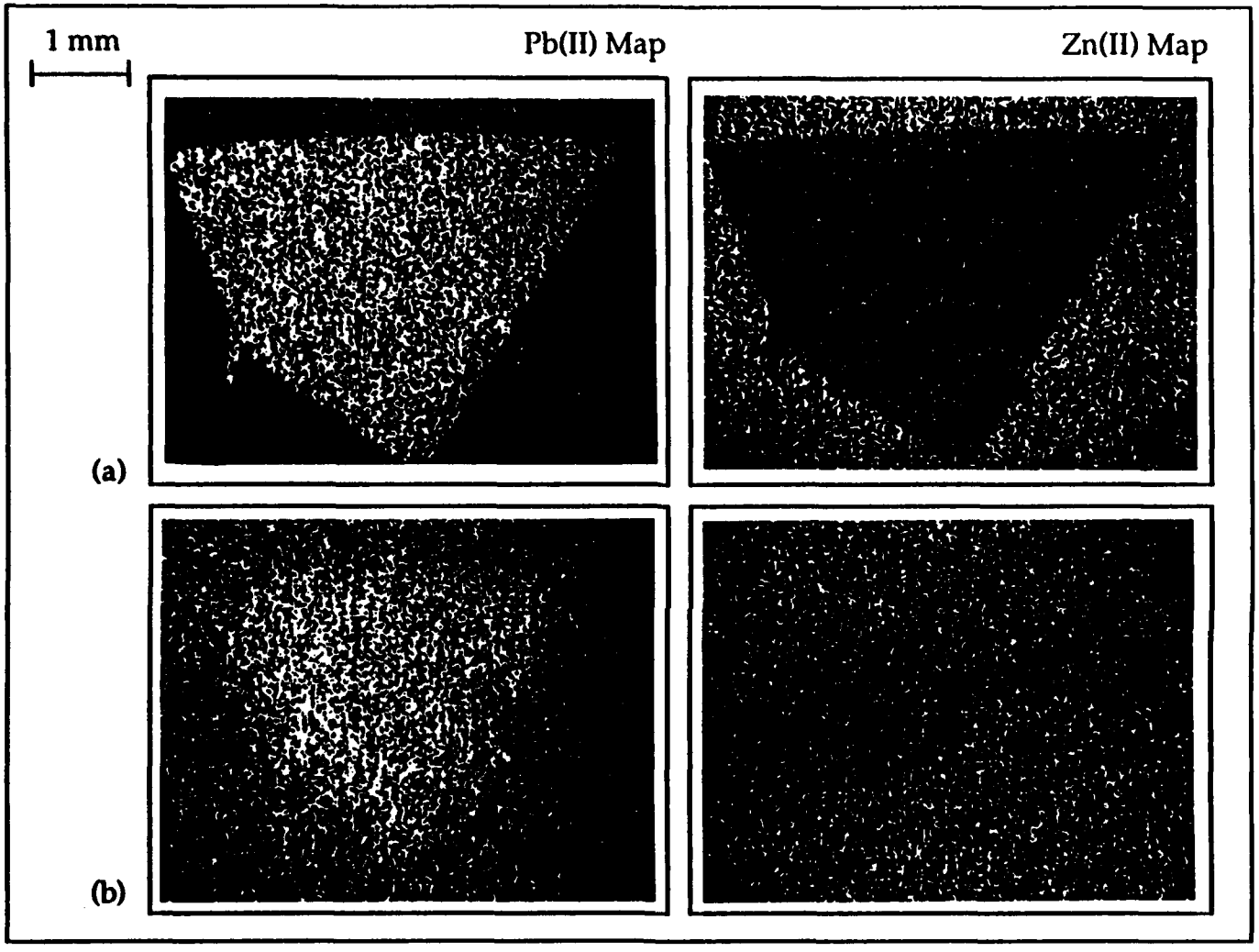

Figure 13 EDX maps of Pb(II) and Zn(II) before (a) and after (b) diffusion in $PbI_2(PEO)_{16}$ / $ZnI_2(PEO)_{16}$ diffusion couple

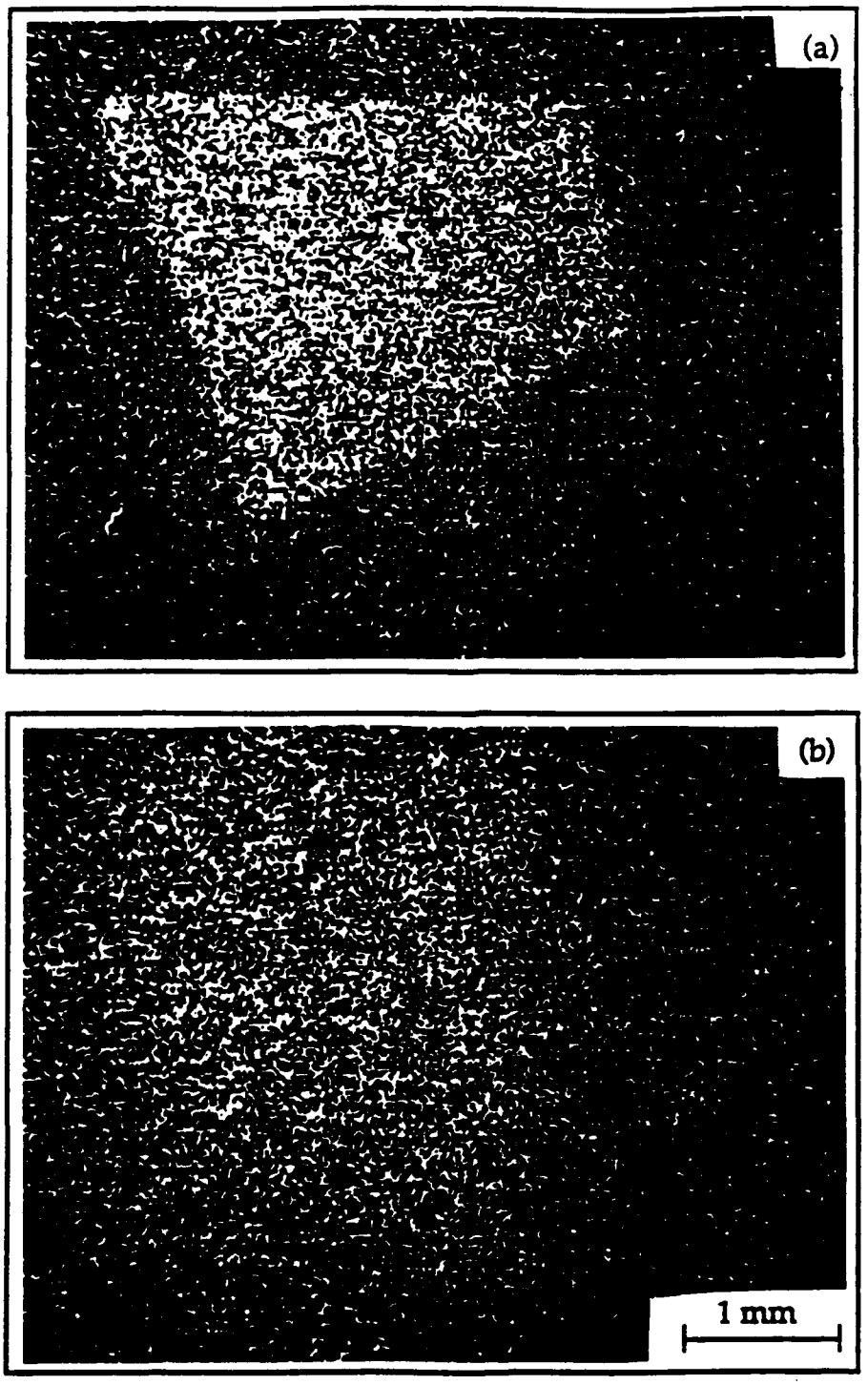

Figure 14 EDX maps of Zn(II) before (a) and after (b) diffusion in $ZnI_2(PEO)_{16}$ / $PbI_2(PEO)_{16}$ diffusion couple

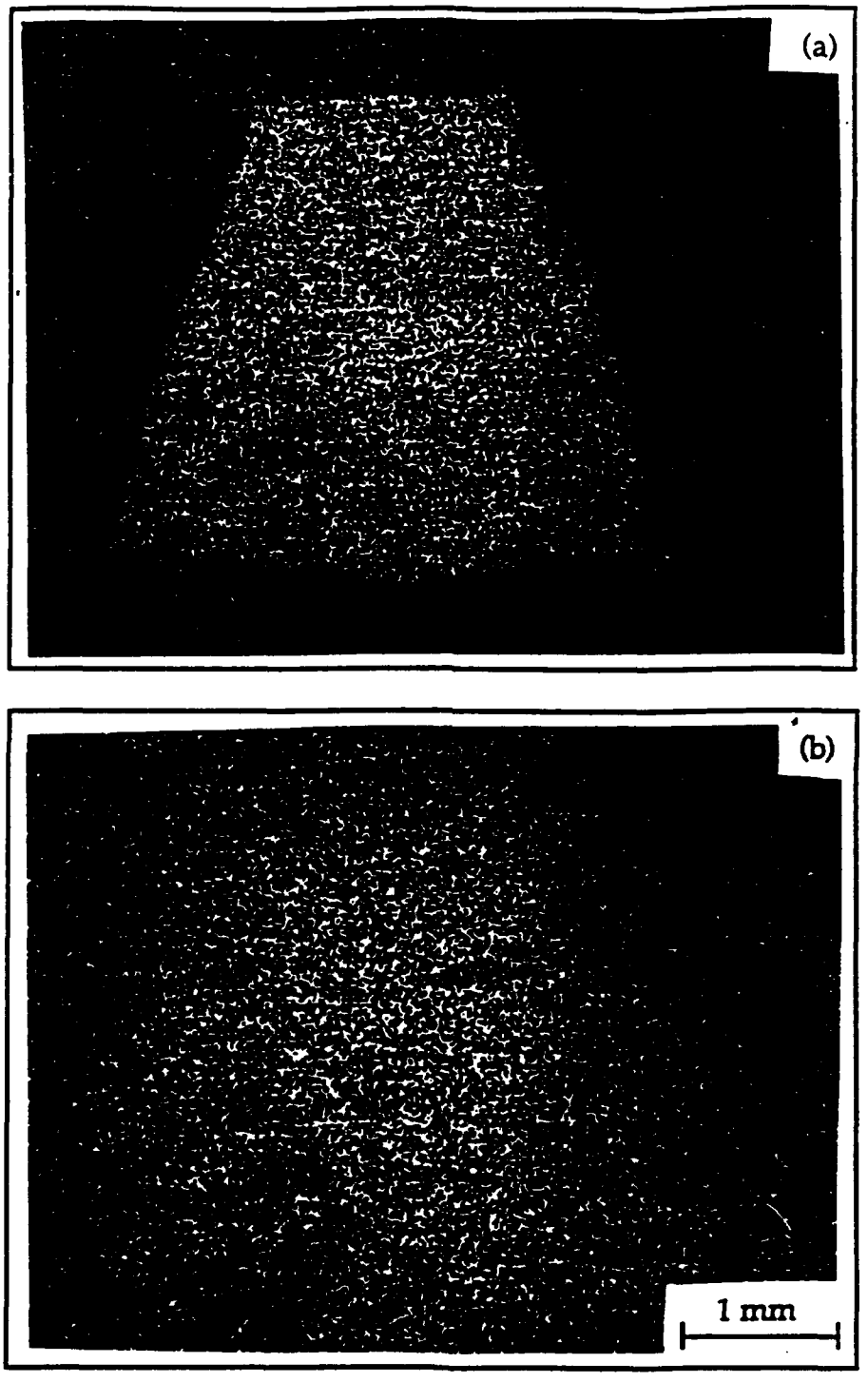

Figure 15 EDX maps of Zn(II) before (a) and after (b) diffusion in $ZnBr_2(PEO)_{16}$ / pure PEO diffusion couple

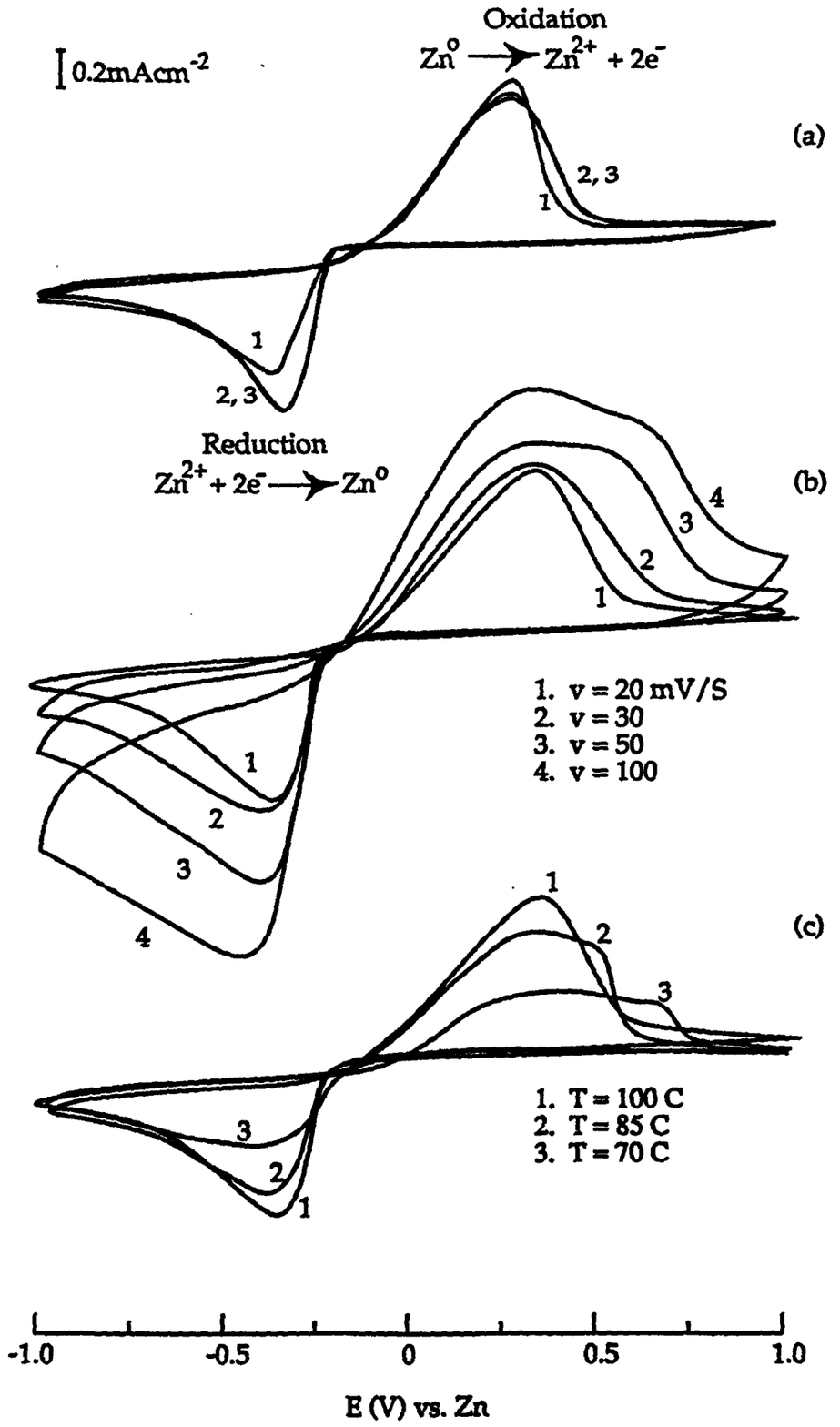

Figure 16 Cyclic Voltammograms of $[0.05ZnBr_2+0.95LiBr](PEO)_{16}$ at 100°C: (a) with a scan rate of 20mV/S (E vs. Zn);(b) with various scan rates; and (c) with a scan rate of 20mV/S at various temperatures

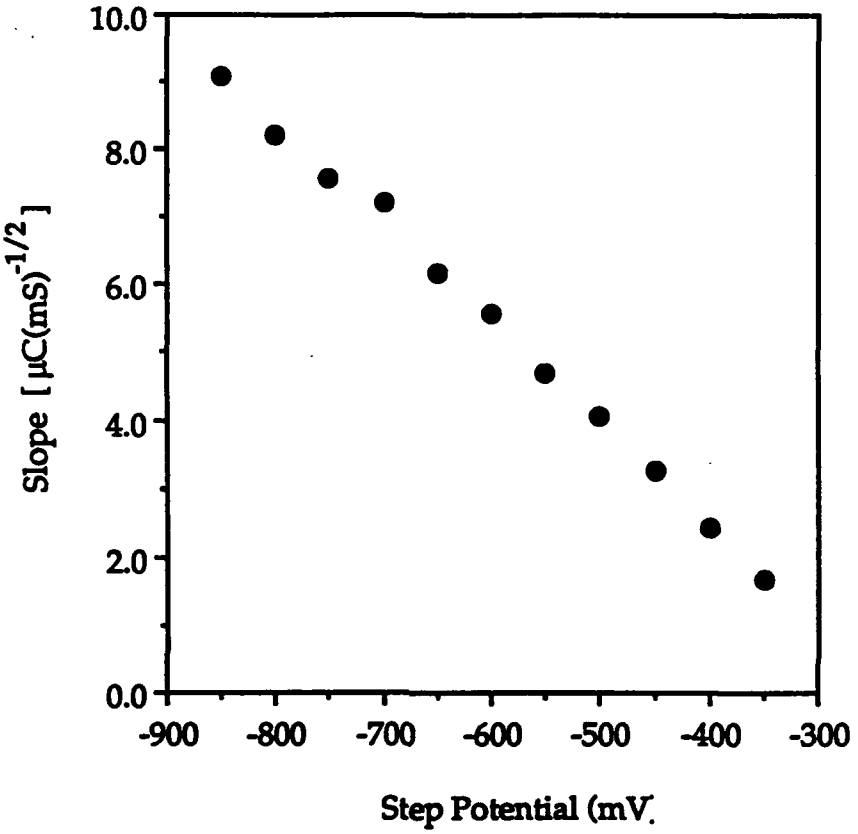

Figure 17 Dependence of the slope of Q vs. $t^{1/2}$ on the applied step potential at 100°C